Journal of Crohn's and Colitis, 2023, **17**, 433–449
https://doi.org/10.1093/ecco-jcc/jjac148
Advance access publication 11 October 2022
Original Article

Autophagy Reduces the Degradation and Promotes Membrane Localization of Occludin to Enhance the Intestinal Epithelial Tight Junction Barrier against Paracellular Macromolecule Flux

Kushal Saha,[a] Ashwinkumar Subramenium Ganapathy,[a] Alexandra Wang,[a] Nathan Michael Morris,[a] Eric Suchanec,[a] Wei Ding,[b] Gregory Yochum,[b] Walter Koltun,[b] Meghali Nighot,[a] Thomas Ma,[a] Prashant Nighot[a]

[a]Division of Gastroenterology and Hepatology, Department of Medicine, The Pennsylvania State University College of Medicine, Hershey, PA 17033, USA
[b]Division of Colon and Rectal Surgery, Department of Surgery, The Pennsylvania State University College of Medicine, Hershey, PA 17033, USA

Corresponding author: Prashant Nighot, Department of Medicine, College of Medicine, Penn State University, Hershey, PA 17033, USA. Tel: 919 607 9833; Email: pnighot@pennstatehealth.psu.edu
Preprint (Biorxiv) doi: https://doi.org/10.1101/2022.04.11.487876

Abstract

Background and Aims: Functional loss of the gut epithelium's paracellular tight junction [TJ] barrier and defective autophagy are factors potentiating inflammatory bowel disease [IBD]. Previously, we showed the role of autophagy in enhancing the intestinal TJ barrier via pore-forming claudin-2 degradation. How autophagy regulates the TJ barrier-forming proteins remains unknown. Here, we investigated the role of autophagy in the regulation of occludin, a principal TJ component involved in TJ barrier enhancement.

Results: Autophagy induction using pharmacological activators and nutrient starvation increased total occludin levels in intestinal epithelial cells, mouse colonocytes and human colonoids. Autophagy induction enriched membrane occludin levels and reduced paracellular permeability of macromolecules. Autophagy-mediated TJ barrier enhancement was contingent on the presence of occludin as *OCLN*$^{-/-}$ nullified its TJ barrier-enhancing effect against macromolecular flux. Autophagy inhibited the constitutive degradation of occludin by preventing its caveolar endocytosis from the membrane and protected against inflammation-induced TJ barrier loss. Autophagy enhanced the phosphorylation of ERK-1/2 and inhibition of these kinases in Caco-2 cells and human colonic mucosa prevented the macromolecular barrier-enhancing effects of autophagy. *In vivo*, autophagy induction by rapamycin enhanced occludin levels in wild-type mouse intestines and protected against lipopolysaccharide- and tumour necrosis factor-α-induced TJ barrier loss. Disruption of autophagy with acute *Atg7* knockout in adult mice decreased intestinal occludin levels, increasing baseline colonic TJ permeability and exacerbating the effect of experimental colitis.

Conclusion: Our data suggest a novel role of autophagy in promoting the intestinal TJ barrier by increasing occludin levels in an ERK1/2 mitogen-activated protein kinase-dependent mechanism.

Key Words: Autophagy; occludin; inflammatory bowel disease; intestinal permeability; tight junction

Graphical Abstract

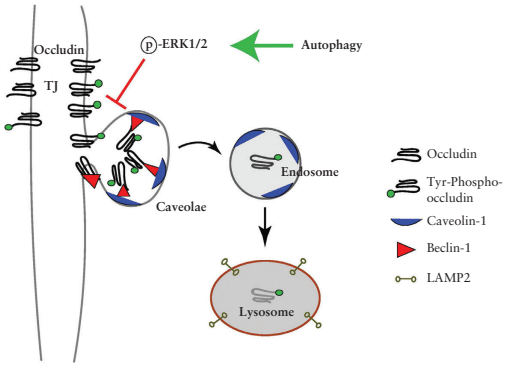

Autophagy, a cell survival mechanism, promotes membrane localization of barrier forming occludin by reducing its endocytosis. Thus, autophagy enhances the epithelial tight junction (T J) barrier against macromolecular flux, in ERK1/2 dependent manner.

1. Introduction

Inflammatory bowel disease [IBD], including ulcerative colitis [UC] and Crohn's disease [CD], is a chronic inflammatory disorder of the gastrointestinal [GI] tract affecting over 1.3% of the adult US population.[1] The aetiology of IBD is multifactorial, but increased permeability of the gut epithelium is a key factor determining the development, pathogenicity and severity of IBD.[2,3] Paracellular transport is a major route of transport for solutes across the gut epithelium and is regulated through cell-to-cell junctions formed by protein aggregates which seal the intermediate space between adjacent epithelial cells. Tight junctions [TJs] occupy the apical surface of the lateral plasma membrane and form a barrier against the free flow of solutes through paracellular space.[3]

Macroautophagy [autophagy] is an evolutionarily conserved mechanism of degradation and recycling of cytosolic contents, serving as a mode of adaptation and protection against cellular stress.[4] The major steps in autophagy are [i] initiation or formation of the isolation membrane, mediated by ULK1/2-ATG13-RB1CC1/FIP200 complex and the BECN1/beclin1-PIK3C3/Vps34-PIK3R4/Vps15-ATG14 complex; [ii] expansion of the phagophore by ubiquitin-like proteins ATG12 and GABARAP/LC3; [iii] autophagosome formation with lipidation of cytosolic LC3-I to LC3-II and binding to the autophagosome membrane; and [iv] fusion of the autophagosome with the lysosome to form an autolysosome which degrades the cargo proteins.[5] Studies have linked defects in autophagy to IBD development, but a mechanistic understanding of the role of autophagy in the regulation of the gut epithelial barrier and the basis of defective autophagy in IBD development remains poorly understood. Being an intracellular degradation pathway, autophagy intersects with endocytic processes in tightly controlled mechanisms,[6,7] and we have previously demonstrated that autophagy promotes the clathrin-mediated degradation of the pore-forming TJ protein claudin-2.[8–10]

Occludin is a MARVEL [MAL-related proteins for vesicle trafficking and membrane link] domain-containing protein family member. It is a tetra-spanning membrane protein with two extracellular loops, one intracellular loop, a short N-terminal domain and a large cytoplasmic C-terminal domain, with which it interacts with the guanylate kinase domain of ZO-1.[11] Several *in vitro* and *in vivo* studies have established the role of occludin as a barrier-forming TJ protein in which depletion of occludin increases macromolecular TJ permeability and overexpression has the opposing effect.[12–15] IBD is characterized by loss of occludin protein and a diminished paracellular barrier,[12–14] further highlighting the importance of this protein. In this study, we investigated the effect of autophagy on occludin expression and the consequential effect on the TJ barrier against paracellular macromolecular flux. Here we report a novel role of autophagy, in which this traditional degradative pathway upregulates occludin protein levels by preventing its constitutive endocytosis and degradation with a resultant enhancement of the TJ barrier against macromolecular flux.

2. Materials and Methods

2.1. Chemicals and antibodies

Rapamycin was purchased from Life Technologies [PH21235], and cycloheximide [C7698], lipopolysaccharide [LPS] O127:B8 [L3129], SBI-0206965 [SML1540], iodoacetamide [I1149] and FITC-tagged 4K dextran [102369855] were obtained from Sigma. Murine tumour necrosis factor [TNF]-α [50349-MNAE] was purchased from SinoBiologicals. Human interferon [IFN]-γ [300-02] and TNF-α [300-01A] were purchased from PeproTech and IL17A [ILA-H5118] from Acrobiosystems. Bafilomycin A1 was purchased from Santa Cruz Biotechnology, [sc-201550], U0126 from TORCS [1144], PD98059 from Calbiochem [513000], and 2-mercaptoethanesulphonic acid [MESNA] from Acros Organics [443150250]. [^{3}H] Inulin [specific activity 100 mCi/mmol] was purchased from American Radiolabelled Chemicals [ART117]. The primary antibodies used included anti-occludin, anti-caveolin-1, anti-ATG7 [autophagy-related 7], anti-SQSTM1/p62, anti-β-actin [ProteinTech; 27260-1-AP, 66067-1-1g, 10088-2-AP, 18420-1-AP and HRP-60008, respectively], anti-beclin-1[Abcam 207612], anti-Y14-phospho caveolin-1, anti-phospho threonine, anti-phospho tyrosine, anti-ERK-1/2 [extracellular signal regulated kinase-1/2], Phospho-p44/42 MAPK [mitogen-activated protein kinase] [Erk1/2] [Thr202/Tyr204] and anti- LAMP2 [Cell Signaling Technologies; 3251S, 9386S, 9411S, 4695S, 4377S and 4906S, respectively]. The anti-rabbit horseradish peroxidase [HRP], anti-mouse HRP, secondary antibodies and all other molecular biology-grade reagents were purchased from various commercial vendors. TaqMan RT primers against human occludin [Hs05465837_g1] and GAPDH [Hs02786624_g1] were purchased from Invitrogen.

2.2. Cell culture

Human intestinal epithelial Caco-2 cells and T84 cells [ATCC] and MDCK-II cells [ECACC] were maintained in Dulbecco's modified Eagle's Medium [DMEM] – High Glucose [Gibco, Cat. No. 11965118] supplemented with 10% heat-inactivated fetal bovine serum and antibiotics at 37°C in a 5% CO_2 incubator. Caco-2 cells were grown on 0.4-μm pore size, 12-mm-diameter filter inserts. The transepithelial electrical resistance [TER] of cells was measured by an epithelial voltohmeter [World Precision Instruments]. Monolayers with a TER of 450–500 Ω/cm^2 were used for experiments. Nutrient starvation was induced in the different cell lines by replacing DMEM with serum-free Earle's Balanced Salt Solution [EBSS] for 24 h for all experiments, unless stated otherwise [Sigma, E3024].

2.3. Determination of Caco-2 paracellular flux

Permeability was determined by measuring the apical-to-basal flux of the paracellular marker inulin [^{3}H, M_r = 5000]. ^{3}H-inulin [1.5 μM, 0.1 μCi] was added to the apical solution and radioactivity was measured in the basal solution at 30 and 60 min using a scintillation counter, as described previously.[15]

2.4. Western blot analysis

Western blot analysis was performed by electrophoresing protein samples in a 4–15% SDS-PAGE gel as discussed by us previously.[9]

2.5. Transmission electron microscopy

Caco-2 cell monolayers grown on a 0.4-μm membrane were subjected to starvation as mentioned above. The control and starvation-induced samples were prepared for immune-gold staining and transmission electron microscopy [TEM].[8]

2.6. Confocal immunofluorescence

Confocal immunofluorescence for occludin, ERK1/2, caveolin-1 and beclin-1 was performed by standard methods. The slides were examined using a Leica SP8confocal fluorescence microscope. Images were processed with LAS X software [Leica Microsystems]. Images are presented as maximum-intensity projections rendered from 30 z-stacks of 0.30 µm. Representatives were of several fields from at least three separate samples.

2.7. Co-immunoprecipitation

Using methods previously discussed, the co-immunoprecipitation (co-IP) experiments were performed using protein G dynabeads from Invitrogen [10004D] according to the manufacturer's protocol.[8]

2.8. Quantitative real-time polymerase chain reaction [PCR]

Cells were dissolved in TRIZol [Invitrogen, 15596026] followed by RNA isolation using the Direct-zol RNA Miniprep Plus Kit [Zymo Research, R2072] according to the manufacturer's instructions. Transcript levels of occludin and GAPDH were quantified as discussed previously.[16]

2.9. Cell surface biotinylation and endocytosis assay

Surface proteins on Caco-2 cells were biotinylated using a Pierce Cell Surface Protein Biotinylation and Isolation Kit [Thermo Scientific, A44390], following the manufacturer's instructions. Cells were then incubated in either normal media or EBSS at 37°C for 0, 3 or 6 h. Isolation and determination of biotinylated protein fractions were performed as previously described.[15]

2.10. CRISPR/Cas9 knockout of occludin, ATG7, ERK-1 and ERK-2

Single guide RNA [sgRNA] targeting the region TGAGCAGCCCCCCAATGTCG of *OCLN*, AAATAA TGGCGGCAGCTACG of *ATG7*, CGGGGAGCCCC GTAGAACC of ERK-1 [*MAPK-3*], CGCGGGCAGG TGTTCGACGT region of ERK-2 [*MAPK-1*] or scrambled sgRNA for control in pCRISPR-LVSG03 [Genecopoeia] was used to generate *OCLN*$^{-/-}$, MAPK *dKO*, *ATG7*$^{-/-}$ and Scr Caco-2 cells.[8] Occludin ORF in pCMV6-AC-GFP [Origene] and corresponding control plasmid were used to transfect Caco-2 cells using Lipofectamine 2000 [Invitrogen, 11668027] as per the manufacturer's instructions.

2.11. Experimental animals

Experimental methodologies used in the study were approved by the Institutional Animal Care and Use Committee [IACUC] of The Pennsylvania State University College of Medicine. Mice were engineered with floxed alleles of *Atg7*, and a transgene expressing the TAM-regulated Cre recombinase fusion protein under control of the ubiquitously expressed ubiquitin C [UBC] promoter was generously provided by Dr Eileen White [Rutgers].[17] Atg7 deficiency was created by providing tamoxifen [Sigma Cat No. T5648; 20 mg/mL suspended in 98% sunflower seed oil and 2% ethanol mixture] to 10-week-old mice as described previously to generate Atg7 conditional knockout mice (cKO).[8] The wildtype C57BL/6J mice [Stock No. 000664, Jackson Laboratory] were treated with rapamycin [40 mg/kg/day for 3 days, i.p injection]. In the dextran sulphate sodium [DSS] model, mice were given 2.5% DSS in drinking water for 7 days.[16] LPS and TNF-α [0.2 µg/kg each] were dissolved in sterile PBS and injected i.p followed by incubation for 12 and 4 h respectively.

2.12. Measurement of paracellular permeability of murine and human colonic tissues

The paracellular permeability of the mice and human intestinal tissues was measured using 0.03-cm^2-aperture Ussing chambers [Physiologic Instruments] and mucosal-to-serosal flux of [^{3}H]-inulin.[18] TER [Ω/cm^2] was calculated from the spontaneous potential difference and short-circuit current.

2.13. Human tissue samples and treatment

The surgically resected, fresh human intestinal tissue samples were obtained from the Department of Surgery, Division of Colon and Rectal Surgery, as per the protocols approved by the Institutional Review Board. Tissues were ascribed as normal or diseased by the Department of Pathology and Laboratory Medicine, Penn State College of Medicine. Tissues were processed[8] and incubated in the presence and absence of 300 nM rapamycin [Alfa Aesar, J62473] with or without 25 µM U0126 or 20 µM PD98059. Human colonic organoids were grown in InstiCult Organoid growth media [Stem Cell, 100-0190] following the manufacturer's instructions. Organoids were differentiated in InstiCult Organoid differentiation media [Stem Cell, 100-0214] and subjected to starvation with EBSS for 24 h in the presence and absence of U0126 or PD98059.

2.14. Statistical analysis

Data are reported as means ± SEM. Data were analysed by using appropriate statistical tests [Sigma Stat, Systat Software].

3. Results

3.1. Autophagy increases cellular occludin and its membrane localization, reducing macromolecular flux across the paracellular space

We have previously shown that autophagy enhances the intestinal TJ barrier by reducing levels of the pore-forming TJ protein claudin-2 through its interaction with the µ-subunit of the clathrin adaptor protein AP2 and autophagy receptor LC3.[8,9] Besides claudin-2, the barrier-forming protein occludin is another major component of the TJ barrier that regulates macromolecular flow across the paracellular space and whose levels diminish in IBD. To study if autophagy affects occludin, we used an established model of nutrient starvation to induce autophagy. We examined occludin levels in colonic epithelial Caco-2 cells upon starvation and found a significant increase in occludin protein levels [Figure 1A and B]. Starvation also increased occludin levels in other epithelial cell lines MDCK-II and T84 [Figure 1C and D], indicating that the starvation-induced increase in occludin protein is not cell-line specific. Next, we examined the effect of known chemical inducers of autophagy on cellular occludin levels. Rapamycin,[9] resveratrol,[19] SMER28,[20] and metformin,[21] which induce autophagy by different mechanisms, reduced the protein levels of the autophagy substrate p62/SQSTM1 and significantly increased occludin protein levels in Caco-2 cells [Figure 1E and F]. Overall, the data show that autophagy-induction in different epithelial cell lines and by different mechanisms increases cellular occludin levels.

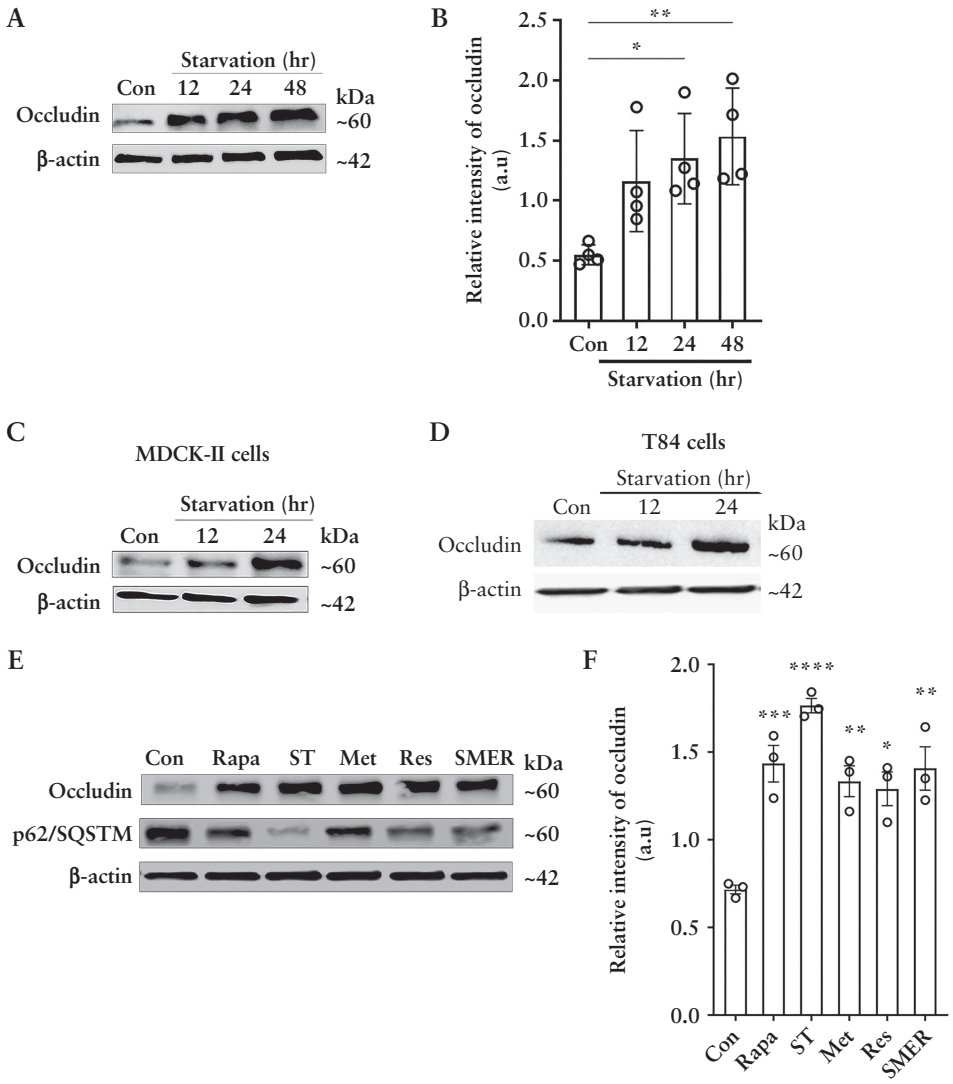

Figure 1. Autophagy enhances cellular occludin levels and enhances the TJ barrier against macromolecular flux. [A] Western blot for Caco-2 occludin levels after starvation. β-Actin is shown as a loading control. [B] Quantification of occludin in panel A using ImageJ software. Blot and densitometry data representative of more than three independent experiments. [C, D] Starvation increased occludin levels in MDCK-II and T84 cells. Blots are representative of three independent experiments. [E] Occludin levels from Caco-2 cells treated with rapamycin [Rapa, 500 nM], EBSS [ST], metformin [MET, 100 μM], resveratrol [RES, 100 μM] and small-molecule enhancer 28 [SMER, 50 μM]. SQSTM/p62 protein degradation indicates autophagy induction. Occludin levels were increased by all the autophagy inducers. [F] Quantification of occludin levels in panel E. Blot and densitometry analysis from three independent experiments. Student's *t*-test or one-way ANOVA with Tukey's post-hoc test. *, $p < 0.05$; **, $p < 0.01$; ***, $p < 0.001$; ****, $p < 0.0001$. a.u = arbitrary units.

Next, we investigated the fate of this increased cellular occludin by cell fractionation analysis and found enhanced levels of occludin in the membrane fractions of Caco-2 cells upon starvation [Figure 2A and B]. Additionally, confocal immunofluorescence [Figure 2C and D] and TEM [Figure 2E] also showed that starvation enhanced the localization of occludin to the TJs. Furthermore, consistent with the importance of Thr phosphorylation of occludin in promoting its TJ localization and the opposing effect of Tyr phosphorylation,[22] we found that occludin immunoprecipitates from Caco-2 cells had a significant reduction of Tyr phosphorylation and a corresponding increase of Thr phosphorylation upon starvation [Figure 2F–H].

We have previously shown that starvation increases TER and decreases the paracellular small solute flux, via claudin-2 degradation.[9] However, occludin is known to regulate the transport of larger, uncharged solutes across the paracellular space otherwise referred to as the leak pathway, which allows movement of solutes of up to ~100 Å diameter in size.[23,24] To examine whether starvation has a barrier-enhancing effect on the leak pathway, we used two markers, inulin [~12 Å diameter] and 4K dextran [~15 Å in diameter] which, owing to their larger size, cannot be transported through the pore pathway for small molecule [~6–8 Å] transport. We found that starvation significantly decreased the paracellular flux of macromolecules inulin [Figure 3A] and 4K dextran [Figure 3B]. Furthermore, the starvation-induced reduction in inulin flux was independent of the autophagy-mediated degradation of claudin-2 since the baseline inulin flux across Scr and *CLDN2*$^{-/-}$ Caco-2 cell monolayers remained unaltered [Figure 3C]. Together, these studies demonstrate that starvation increases the levels and TJ localization of the occludin protein and enhances the TJ barrier against macromolecule flux.

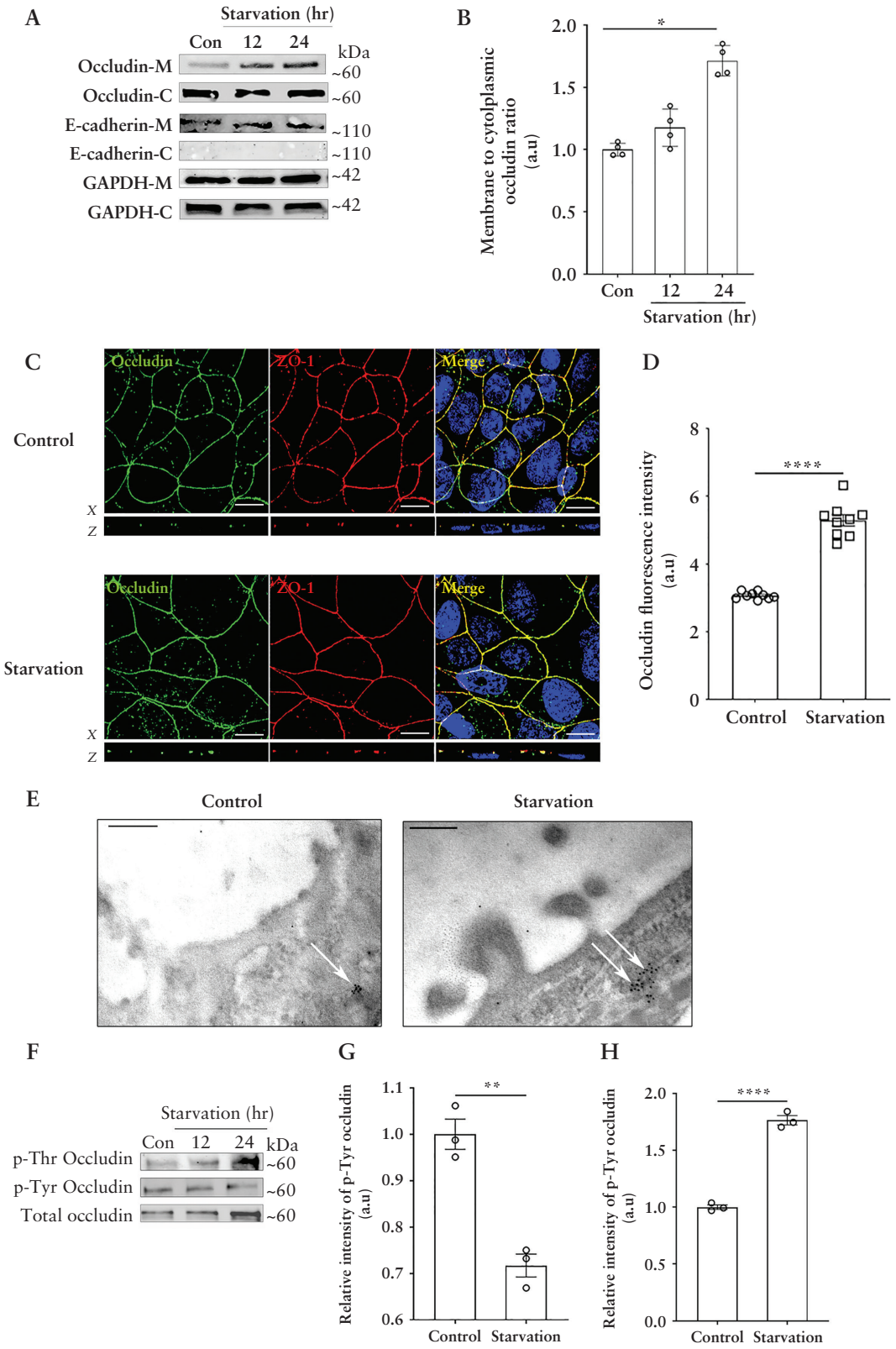

Figure 2. Starvation enhances the membrane localization of occludin. [A] Starvation increased the relative presence of occludin in the membrane fraction. M: membrane; C: cytoplasm. E-cadherin is shown as a marker for the cell membrane and GAPDH as a loading control. [B] Quantification of the membrane to cytoplasmic occludin ratio. Representation of three or more independent experiments. [C] Starvation increased the presence of occludin [green] on the cell membrane at the TJs. ZO-1 [red]. Nuclei: blue. White scale bar = 5 µm. [D] Quantification of occludin fluorescence intensity from panel C. Image and fluorescence quantification data representative of three independent experiments. [E] Immunogold transmission electron microscopy revealed an increased presence of occludin [black dots] at the TJs [white arrows] of Caco-2 cells upon starvation. Image representative of three independent experiments and > 30 fields per experiment. Black scale bar = 200 nm. [F] Starvation decreases the tyrosine phosphorylation of occludin while simultaneously enhancing its threonine phosphorylation. [G, H] Densitometric quantification of Tyr and Thr phosphorylated occludin, respectively, after 24 h of starvation. Blot and densitometry analysis from three independent experiments. Student's *t*-test or one-way ANOVA with Tukey's post-hoc test. *, $p < 0.05$; **, $p < 0.01$; ****, $p < 0.0001$.

3.2. Autophagy reduces occludin endocytosis and enhances the protein half-life

We next examined the possible mechanism underlying the starvation-mediated upregulation of occludin protein. We observed no significant difference in occludin transcript levels in Caco-2 cells upon starvation [Figure 4A]. Thus, we investigated the possibility of reduced occludin protein degradation. In contrast to a temporal reduction of the occludin protein in the control samples in the presence of the protein synthesis inhibitor cycloheximide, occludin protein levels in the starved Caco-2 cell samples showed no significant change, suggesting that starvation protects occludin from degradation [Figure 4B]. Occludin undergoes caveolar endocytosis by interacting with caveolin-1, the primary protein component of caveolar structures.[15,25] Additionally, we have reported the autophagy-independent role of the Atg6/Beclin-1 protein in the constitutive caveolar endocytosis and lysosomal degradation of occludin.[26] Therefore, we probed occludin immunoprecipitates from control and starved Caco-2 cells for caveolin-1, beclin-1 and the lysosomal marker LAMP-2. Co-IP showed a temporal reduction in the interaction of occludin with all three proteins upon starvation [Figure 4C and D]. We next assessed if this reduction of occludin degradation and association with caveolin-1 is a consequence of starvation-induced abrogation of the global caveolar endocytosis pathway. Studies have reported that caveolin-mediated endocytosis requires the phosphorylation of the caveolin-1 protein on the Y-14 residue,[23] and hence we determined the level of phospho-caveolin-1 [pY-14-Cav-1] in Caco-2 cells and observed an increase during starvation, indicating that the global caveolae-mediated endocytosis remains unaffected during autophagy induction [Figure 4E]. In a complementary approach, we also assessed the uptake of cholera toxin, which is known to undergo caveolar endocytosis, by control and starved Caco-2 cells and observed no difference in the ability of the cells to endocytose the toxin between control and starved samples [data not shown].

Next, we directly assessed the effect of starvation on occludin endocytosis using biotin labelling.[15,27] For this, after biotinylation of the membrane proteins, the Caco-2 cells were

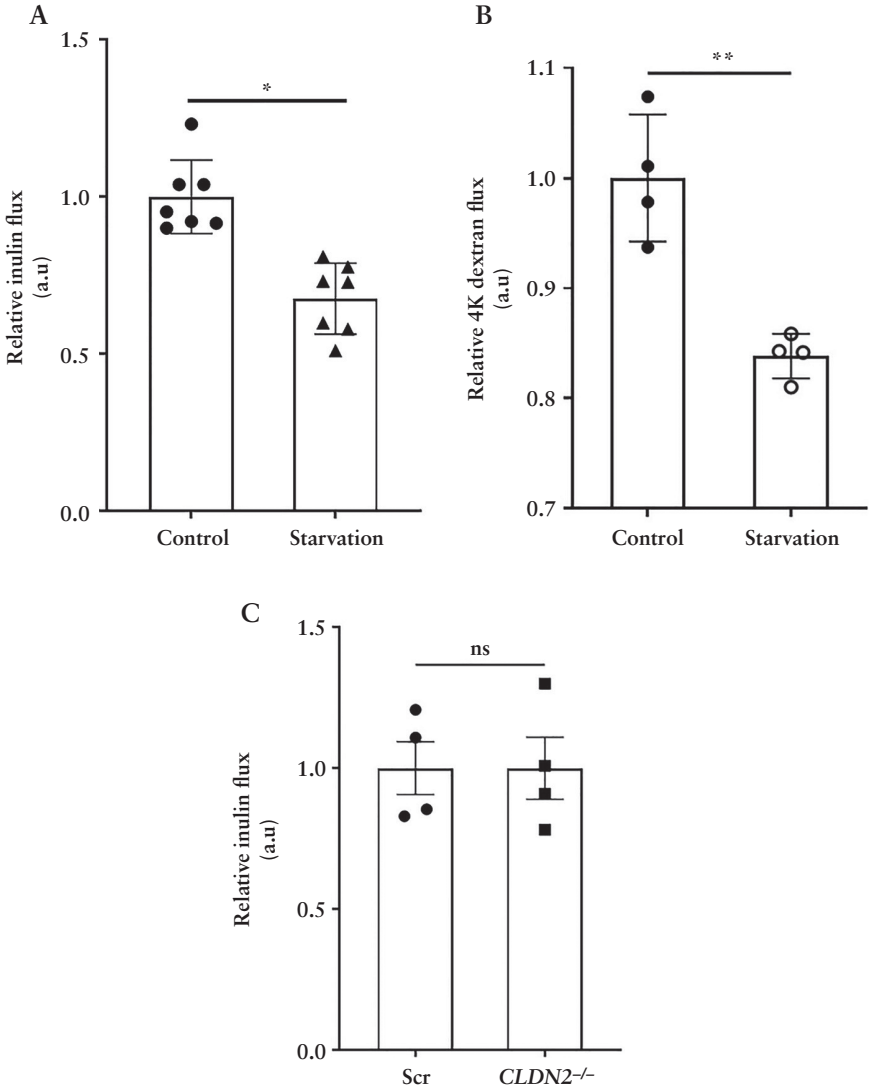

Figure 3. Starvation enhances the paracellular TJ barrier. Starvation reduces the apical to basolateral paracellular flux of inulin [A] and 4K dextran [B] across Caco-2 cell monolayers. [C] Deletion of claudin-2 did not affect the flux of inulin. Data are representative of at least three independent experiments. Student's *t*-test. *, $p < 0.05$; **, $p < 0.01$; ns, non-significant.

subjected to starvation, followed by removal of all surface biotin and isolation of endocytosed biotinylated proteins. We observed increased levels of biotinylated occludin in control cell lysates compared to starved cells, indicating reduced endocytosis of occludin after starvation [Figure 4F and G]. We have previously shown that treating Caco-2 cells with caveolin-1 scaffold domain [CSD] peptide induces occludin degradation by enhancing its endocytosis in caveolar pits.[26] Assessment of occludin levels in Caco-2 cells showed a significant reduction upon CSD treatment alone, but starvation prevented CSD-mediated reduction in occludin levels [Figure 4H]. Furthermore, confocal imaging showed increased co-localization between occludin and caveolin-1 upon CSD treatment which was absent in the cells subjected to starvation [Figure 4I]. Thus, starvation selectively protected occludin from endocytosis and degradation by disrupting its association with caveolin-1.

3.3. Starvation-induced enhancement of the TJ barrier is autophagy and occludin dependent

We next confirmed the role of autophagy on starvation-induced upregulation in occludin levels and the TJ barrier enhancement. We found that autophagy inhibitors, bafilomycin A1 or SBI-0206965, prevented the starvation-induced

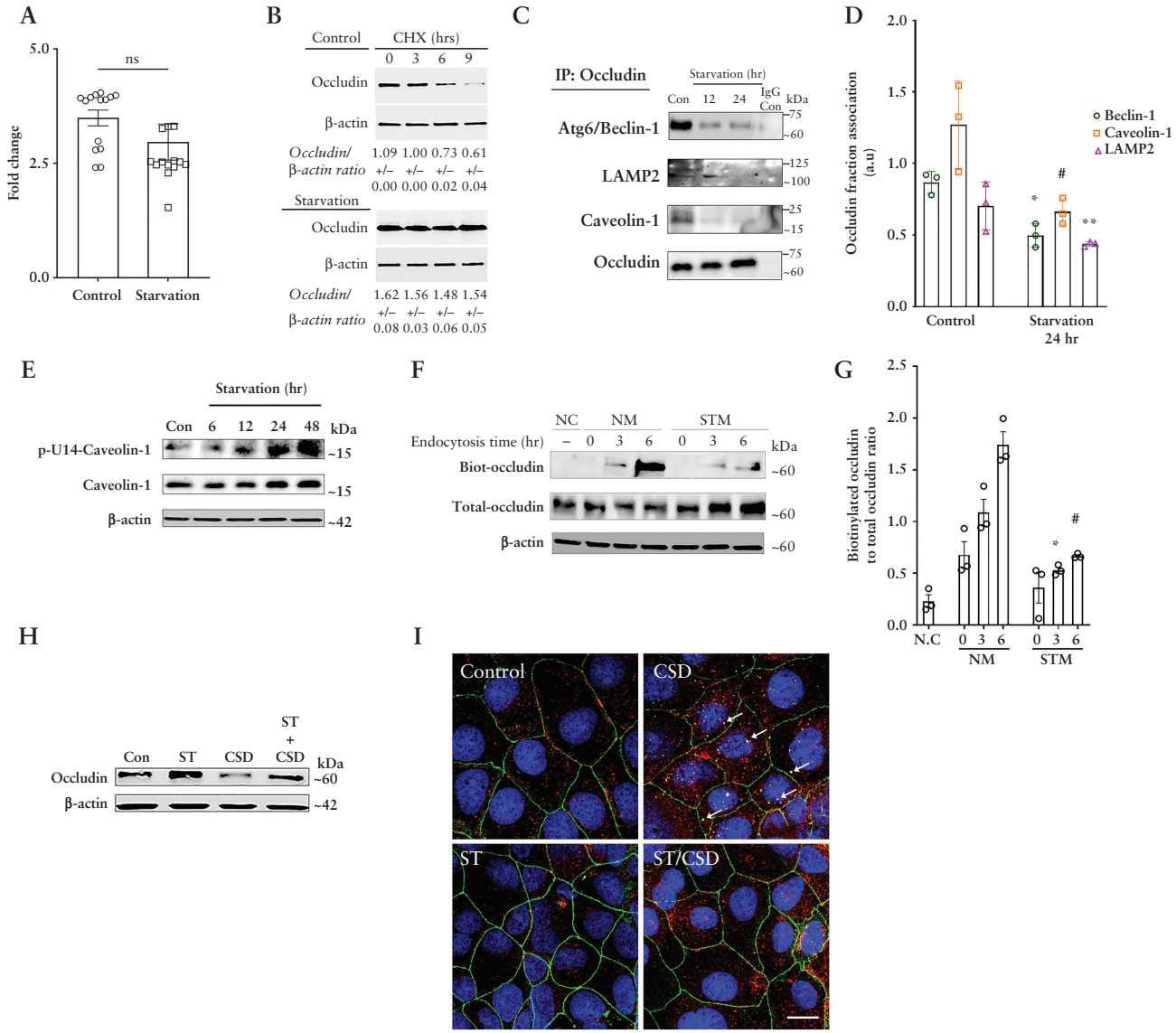

Figure 4. Autophagy enhances the half-life of occludin and reduces its constitutive degradation. [A] The mRNA levels of occludin did not alter significantly upon starvation. [B] Cycloheximide did not affect occludin levels upon starvation. Quantification of relative occludin levels from three independent experiments is denoted in numbers as mean ± SEM. [C] Co-immunoprecipitation studies showed decreased association of occludin with beclin-1, caveolin-1 and the lysosomal marker LAMP-2 after starvation. The negative control includes immunoprecipitation with control IgG. [D] Quantification of beclin-1, caveolin-1 and LAMP2 in occludin immunoprecipitates from panel B. $n = 3$. *, # and **, $p < 0.01$ vs respective controls. [E] Starvation enhanced the levels of Y-14 phosphorylated caveolin-1. [F] Starvation reduced the endocytosis of membrane-bound, biotinylated occludin. NC, negative control; NM, normal media; STM, starvation media. [G] Quantification of biotin-labelled to total occludin ratio from panel D. $n = 3$. [H] Starvation protects occludin from caveolin-1 scaffolding domain [CSD] peptide [5 μM]-induced occludin degradation. $n = 3$ independent experiments. [I] Starvation reduced the CSD-induced co-localization [yellow, white arrows] between occludin [green] and caveolin-1 [red]. Representative of three independent experiments. White scale bar = 5 μm. Student's *t*-test or one-way ANOVA with Tukey's post-hoc test. *, $p < 0.05$; **, $p < 0.01$; ***, $p < 0.001$; ****, $p < 0.0001$; ns, not significant.

increase in occludin levels [Figure 5A and B]. Inhibition of autophagy with bafilomycin A1 or SBI-0206965 also prevented the starvation-mediated reduction in the paracellular inulin flux [Figure 5C]. To further verify the role of autophagy in TJ barrier enhancement and occludin upregulation, we used CRISPR/Cas9-mediated *ATG7* knockout [*ATG7*$^{-/-}$] to disrupt the autophagy pathway in Caco-2 cells [Figure 5D].[8] To this end, we observed no changes in occludin levels upon starvation in *ATG7*$^{-/-}$ cells compared to Caco-2 cells and non-target, scrambled [Scr] guide RNA transfected Caco-2 cells [Figure 5E and F]. Additionally, unlike Scr cells, starvation in *ATG7*$^{-/-}$ cells did not reduce the inulin flux [Figure 5G], nor the CSD-induced co-localization of occludin and caveolin-1 [Figure 5H–J]. Together, these data demonstrate that the autophagy pathway plays a key role in the upregulation of occludin protein levels and enhancement of the paracellular

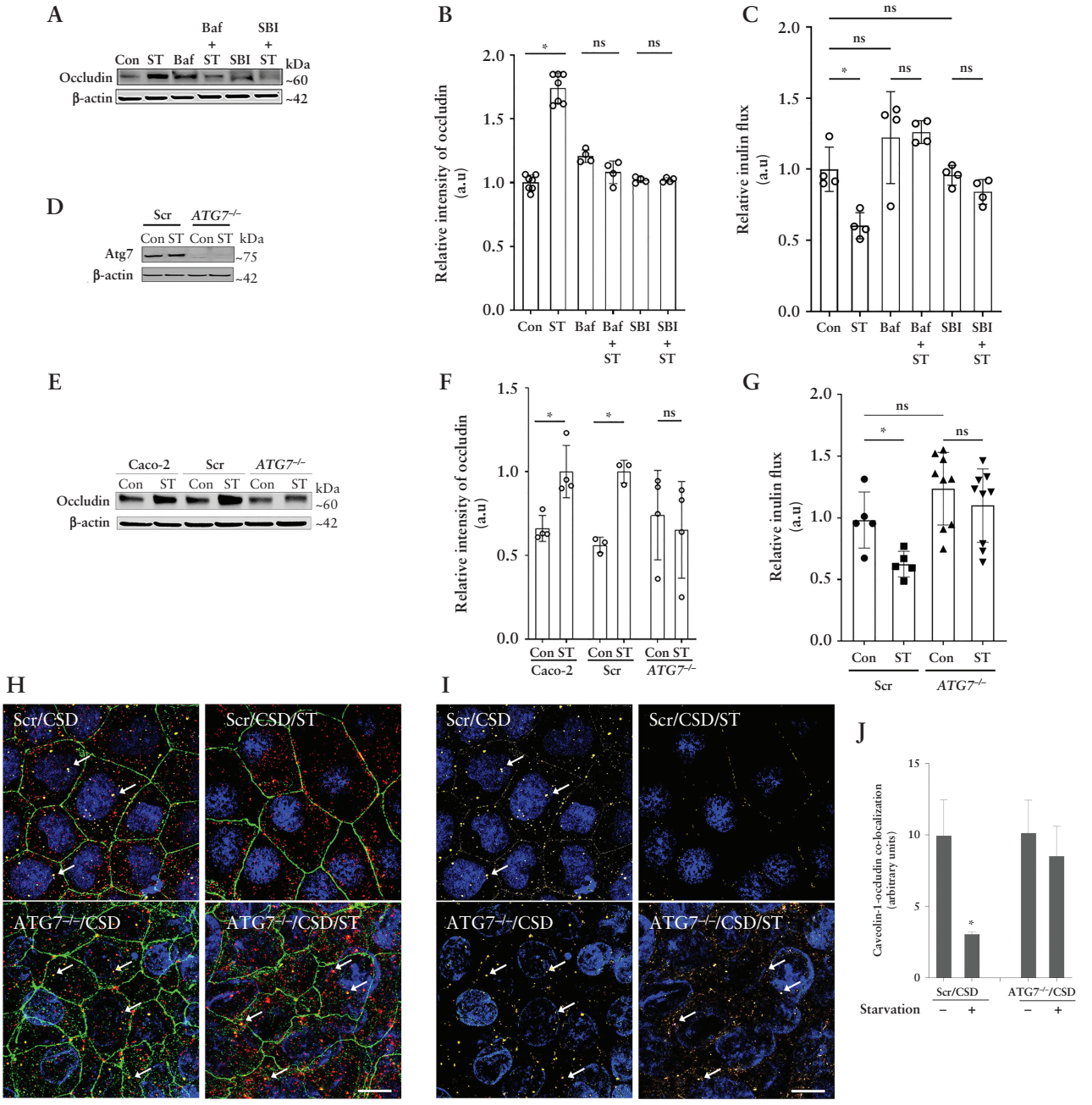

Figure 5. Role of autophagy and occludin in the starvation-induced enhancement of the TJ barrier. [A] Autophagy inhibitors bafilomycin A [Baf, 20 nM] or SBI-0206965 [SBI, 30 μM] prevented the starvation-induced increase in occludin levels. [B] Quantification of occludin levels in panel A. $n > 3$ in each group. [C] Baf and SBI prevented the starvation-induced reduction in inulin flux. [D] Western blot showing the efficacy of CRISPR/Cas9-mediated knockout of *ATG7* in Caco-2 cells. [E] Starvation did not up-regulate occludin levels in *ATG7*$^{-/-}$ cells. [F] Quantification of occludin protein in panel E. [G] Starvation did not reduce paracellular inulin flux in *ATG7*$^{-/-}$ cells. [H] Starvation did not prevent the co-localization [white arrows] between occludin [green] and caveolin-1 [red] upon CSD treatment in the *ATG7*$^{-/-}$ cells. [I] Subtracted image of occludin and caveolin-1 co-localization [yellow] shown with white arrows in Scr and *ATG7*$^{-/-}$ cells upon CSD treatment with and without starvation. White scale bar = 5 μm. [J] Quantification of occludin and caveolin-1 co-localization in Scr and *ATG7*$^{-/-}$ cells upon CSD treatment; $n > 6$ independent experiments. Student's *t*-test or one-way ANOVA with Tukey's post-hoc test. *, $p < 0.05$; ns, non-significant.

barrier against macromolecular flux via the reduction in caveolae-mediated occludin endocytosis.

To test whether occludin is needed for the starvation-induced TJ barrier enhancement against macromolecular flux, we utilized CRISPR/Cas9 to generate occludin knockout [$OCLN^{-/-}$] Caco-2 cells [Figure 6A]. We observed that starvation significantly increased the TER in $OCLN^{-/-}$ cells [Figure 6B], but the inulin flux in the $OCLN^{-/-}$ cell monolayers remained unchanged upon starvation [Figure 6C]. Together, these data demonstrate the key role of occludin in the autophagy-induced paracellular macromolecule permeability reduction.

3.4. Starvation-induced enhancement of cellular occludin levels and TJ barrier is mediated by ERK-1/2

Previous studies have shown the critical role of the MAPK pathway in both autophagy[28] and membrane localization of TJ proteins.[29] Additionally, our analysis of the Caco-2 proteome also indicated links between the ERK1/2 kinases, occludin, autophagy and associated endocytic components [Figure 7A]. Therefore, we tested the role of ERK1/2 in the starvation-induced enhancement of the TJ barrier. Starvation activated ERK-1 and 2, as evidenced by the increased phosphorylation of these kinases [Figure 7B and C]. Pharmacological inhibition of the ERK1/2 kinases with either U0126 or PD98059 prevented the starvation-induced reduction of inulin flux [Figure 7D]. In contrast, p38 or JNK MAPK inhibition [SB 202190 and SP600125, respectively] did not affect the autophagy-induced reduction in macromolecular flux [data not shown]. Next, we employed CRISPR/Cas9 to knock out the ERK-1 and 2 genes in Caco-2 cells [*dKO*] [Figure 7E]. Though like the non-target Scr cells, the TER significantly increased in the *dKO* cells upon starvation [Figure 7F], starvation failed to reduce the inulin flux in the *dKO* cells [Figure 7G]. This observation supports the presence of distinct mechanisms of autophagic regulation of the pore and leak pathways.

Next, we assessed the effect of ERK1/2 deletion on occludin endocytosis. The occludin immunoprecipitates showed that starvation failed to reduce the association of occludin with caveolin-1, beclin-1 and LAMP-2 in the *dKO* cells [Figure 8A and B]. Furthermore, in the *dKO* cells, starvation did not prevent the association between occludin and caveolin-1 upon CSD treatment [Figure 8C and D]. Upon assessing the phosphorylation status of occludin in the Scr and *dKO* cells, we observed increased Thr phosphorylation of the protein upon starvation in both cell lines [data not shown]. However, compared to Scr cells, the *dKO* cells exhibited higher baseline levels of Tyr phosphorylation, which further increased upon starvation [Figure 8E]. Thus, these studies demonstrate the essential role of the ERK-1/2 kinases in regulating the phosphorylation state of phosphorylation state of occludin, thereby maintaining its stability at TJs and protecting it from degradation and thereby regulating the macromolecular flux upon autophagy induction.

3.5. Occludin protects against inflammation-induced barrier loss

We next assessed if the starvation-induced upregulation of occludin protects the epithelial TJ barrier against immune injury. Increased production of IFN-γ, TNF-α and IL-17A by hyperactive gut-resident lymphocytes and loss of the gut epithelial barrier are hallmarks of IBD.[30,31] Therefore, we assessed the effect of starvation on the cytokine-induced barrier loss. For this, filter-grown Caco-2 cells were incubated with a cytokine cocktail comprising the three cytokines added to the basolateral side. Cytokine treatment significantly reduced occludin levels, which was prevented by starvation [Figure 9A and B]. Cytokine addition progressively decreased the TER over time compared to control cells, but incubation of Caco-2 cells with starvation media prevented this cytokine-induced loss of TER [Figure 9C]. Additionally, the macromolecular inulin flux which is primarily related to occludin was significantly increased upon cytokine treatment and was prevented by starvation [Figure 9D]. We next assessed the effect of exogenous occludin overexpression in the cytokine-induced paracellular TJ barrier loss. In a similar cytokine treatment on Caco-2 cells overexpressing occludin [Caco-2^{OCLN}] [Figure 9E and F], we did not observe loss of the paracellular TJ barrier [Figure 9G] compared to empty vector control [Caco-2^{Scr}]. Epithelial occludin has been shown to impact susceptibility for apoptosis under inflammatory conditions.[32] Autophagy-mediated or exogenously up-regulated occludin levels in Caco-2 cells, however, did not show increased apoptosis upon cytokine treatment [Figure 9H]. Collectively, these data highlight the protective role of the increased levels of occludin in maintaining the TJ barrier during cytokine injury.

3.6. Autophagy induction protects against LPS and TNF-α-induced intestinal injury *in vivo*

Next, we examined the protective role of autophagy-induced increase in occludin levels *in vivo*. Intraperitoneal rapamycin injection in WT mice successfully induced autophagy in the mouse colon, as evidenced by the degradation of the autophagy

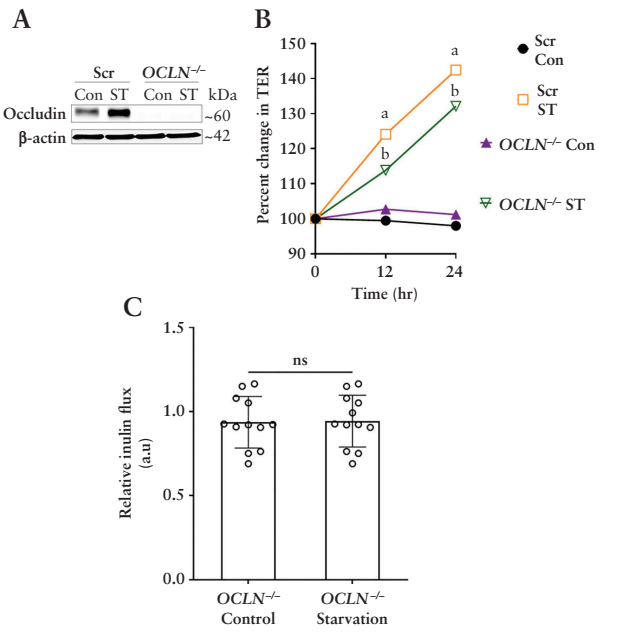

Figure 6. Autophagy-induced enhancement of the TJ barrier is dependent on occludin. [A] Western blot showing the efficacy of CRISPR/Cas9-mediated knockout of occludin in Caco-2 cells. [B] Starvation significantly increased the TER in both Scr and $OCLN^{-/-}$ Caco-2 cell monolayers. [C] Inulin flux remained unchanged upon starvation in the $OCLN^{-/-}$ cells. Data are representative of more than four independent experiments. Student's *t*-test; [a, b], $p < 0.05$ vs control; ns, non-significant.

substrate p62/SQSTM1. Rapamycin administration also increased colonic epithelial occludin protein levels [Figure 10A and B], and reduced colonic inulin flux [Figure 10C]. We next tested the effect of this rapamycin-induced autophagy and occludin upregulation in intestinal injury models. LPS, major components of gram-negative bacterial cell walls, and TNF-α, a pro-inflammatory cytokine, are known to elicit intestinal injury and cause loss of the occludin-associated TJ

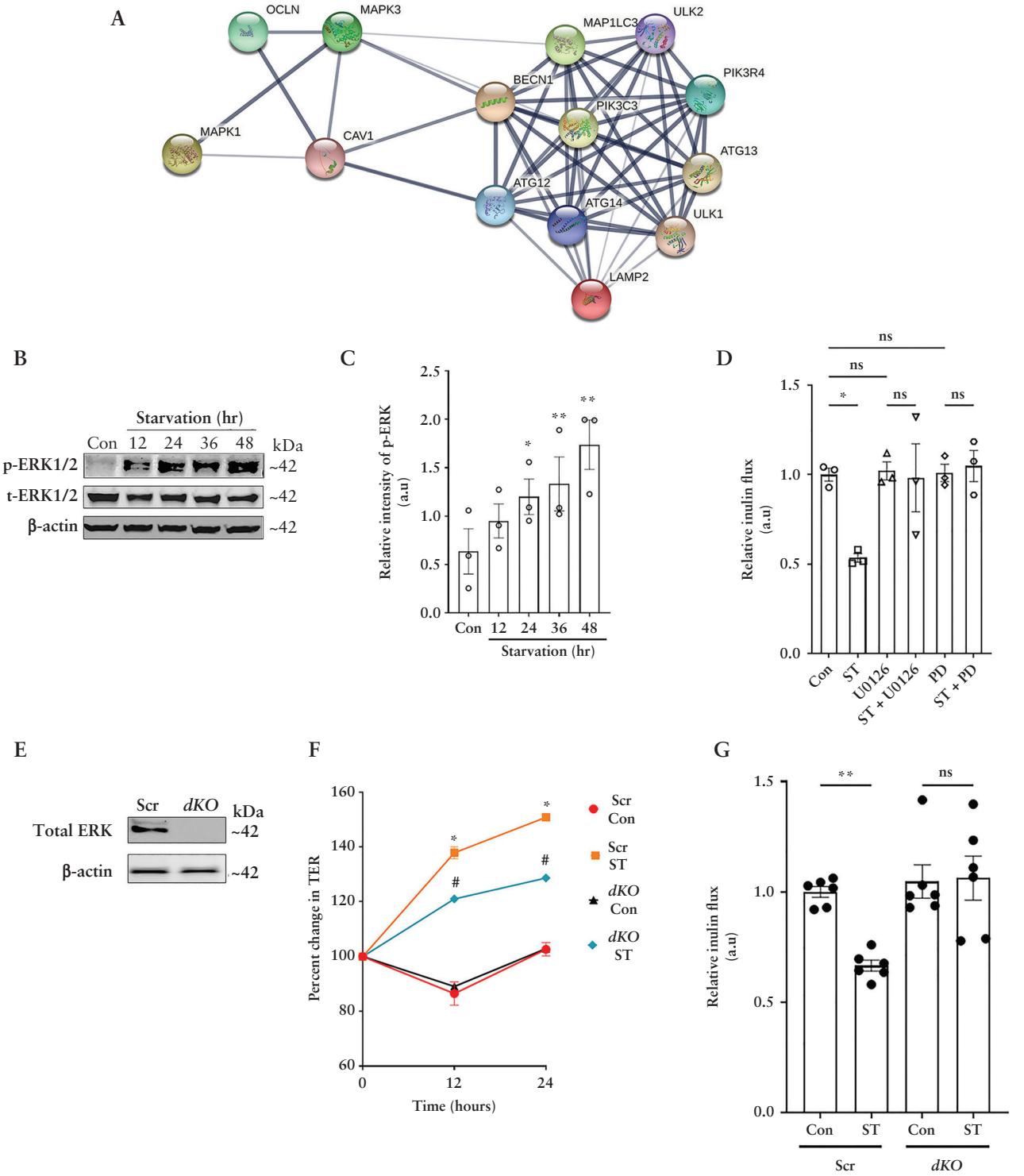

Figure 7. The MAPK proteins ERK-1 and ERK-2 are essential for the autophagy-induced upregulation of occludin. [A] STRING analysis of the Caco-2 protein interactome shows crossover between MAPK proteins ERK1/2, occludin, caveolin-1 and the autophagy cluster. [B] ERK1/2 phosphorylation increased after starvation. [C] Quantification of phospho-ERK1/2 levels in panel B. Blot and densitometric quantification from three independent experiments. [D] Inhibition of ERK1/2 activation with U0126 [25 μM] or PD98059 [20 μM] prevented the starvation-induced reduction in inulin flux. Data represent three independent experiments. [E] Efficacy of CRISPR/Cas9-mediated knockout of the ERK-1 and ERK-2 in Caco-2 [*dKO*] cells. [F] Starvation increased the TER of both Scr and *dKO* Caco-2 cell monolayers, but did not change the inulin flux in ERK deficient *dKO* cells [G]. Data from six independent experiments. One-way ANOVA with Tukey's post-hoc test. *, # and **, $p < 0.05$.

barrier.[25,34,35] Intraperitoneal LPS injection in WT mice led to a significant loss in colonic occludin levels which was prevented upon autophagy-inducer rapamycin treatment [Figure 10A, B, and D]. Loss of occludin levels in LPS-injected mice was accompanied by increased colonic inulin permeability, and rapamycin significantly protected against LPS-induced increase in colonic TJ permeability [Figure 10C]. Similar to LPS, intraperitoneal TNF-α administration increased the mouse colonic permeability of inulin [Figure 10E] which was significantly attenuated by rapamycin. Rapamycin also prevented the TNFα-induced increase in occludin–caveolin-1 association in mouse colonocytes [Figure 10F]. Intraperitoneal rapamycin administration also prevented the LPS- and TNF-α-induced increase in inulin flux in mouse small intestine [data not shown].

To confirm the role of autophagy in the TJ barrier protection conferred by rapamycin in the LPS and TNF-α models described above, we performed the same experiments in autophagy-deficient *atg7* cKO mice. Acute deletion of *Atg7* in adult mice disrupted autophagy[8] and reduced baseline occludin protein levels in the mice colon [Figure 11A and B]. The *atg7* cKO mice also showed increased baseline colonic inulin flux compared to $Atg7^{fl/fl}$ mice [Figure 11C]. Both LPS and TNF-α significantly increased colonic inulin flux in *atg7* cKO mice compared to $Atg7^{fl/fl}$ mice [Figure 11D and E]. Moreover, unlike the WT mice, rapamycin had no protective effect against the LPS- and TNF-α-induced increase in colonic inulin permeability in autophagy-deficient *atg7* cKO mice [Figure 11D and E]. Finally, consistent with a previous report,[36] and our recent data showing increased susceptibility of the *atg7* cKO mice to experimental DSS colitis compared to $Atg7^{fl/fl}$,[8] the *atg7* cKO DSS mice also showed remarkably increased colonic large molecule flux compared to $Atg7^{fl/fl}$ DSS mice [Figure 11F]. In sum, these studies strongly underscore the role of autophagy-mediated increases in occludin levels against inflammation-associated TJ barrier loss.

3.7. Autophagy upregulates occludin levels and enhances the TJ barrier in human colonic explants and colonoids in an ERK1/2-dependent process

We next assessed the role of autophagy on occludin levels in the human colon. Rapamycin increased occludin levels in explant cultures from surgically resected diseased and adjoining normal colonic tissues from CD patients [Figure 12A and B].

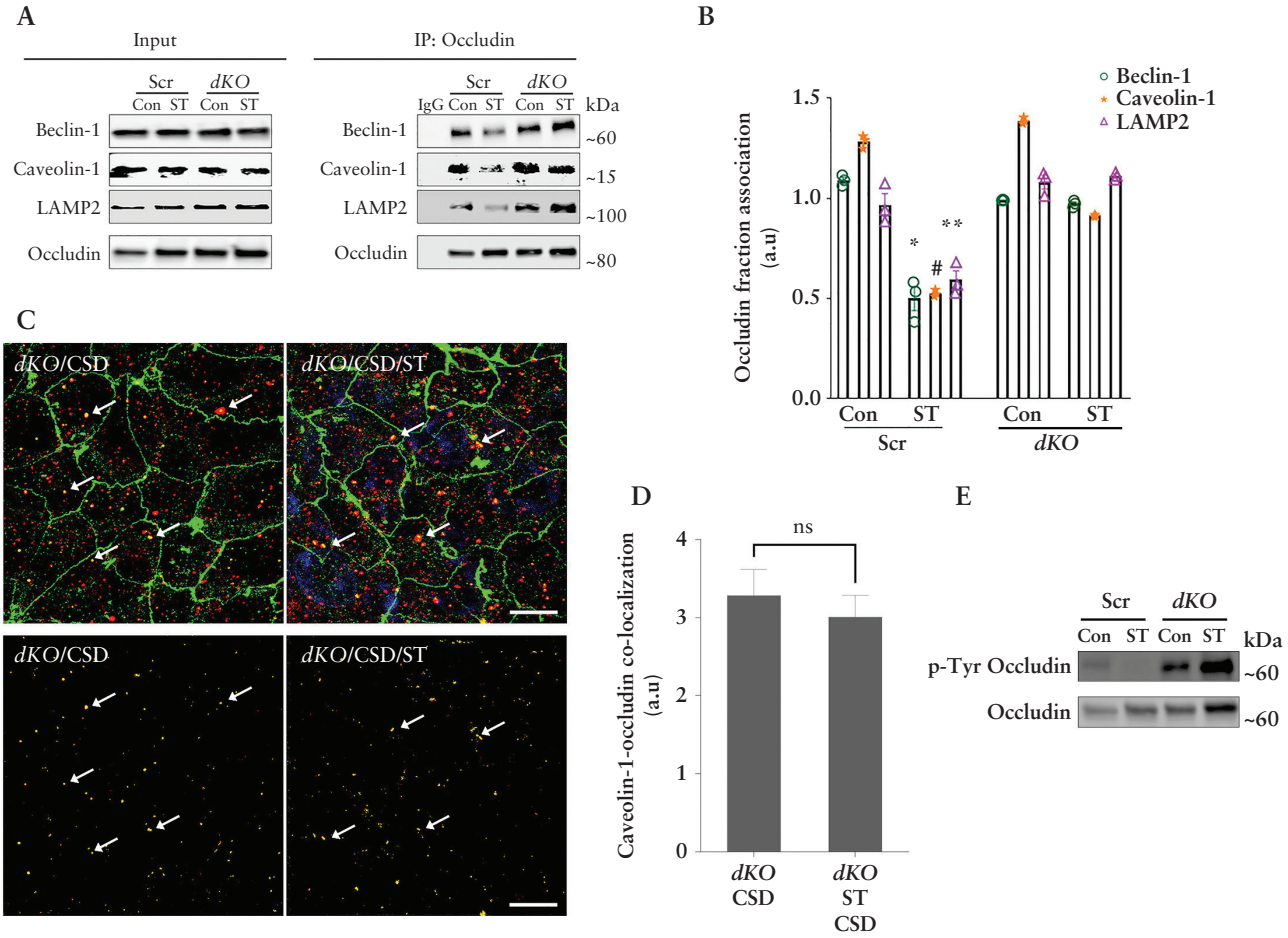

Figure 8. Autophagy fails to protect occludin from endocytosis in the absence of the ERK1/2 kinases. [A] Under co-immunoprecipitation, autophagy did not reduce the interaction of occludin with LAMP-2, beclin-1 and caveolin-1 in the ERK kinase *dKO* cells. [B] Quantification of beclin-1, caveolin-1 and LAMP-2 in occludin immunoprecipitates from panel A. Blot and quantification data represent three independent experiments. [C] Starvation did not prevent the co-localization [white arrows] between occludin [green] and caveolin-1 [red] upon CSD treatment in the *dKO* cells. White scale bar = 5 μm. [D] Quantification of occludin and caveolin-1 co-localization [white arrows] in *dKO* cells upon CSD treatment in the presence or absence of starvation. [E] *dKO* cells have higher baseline levels of Thr phosphorylated occludin, which unlike in Caco-2 and Scr cells, increases upon starvation. One-way ANOVA with Tukey's post-hoc test. *, # and **, $p < 0.05$ Scr Con vs Scr ST; ns, non-significant.

Similarly, autophagy induction with incubation in starvation media or treatment with rapamycin increased occludin immunofluorescence in human colonic stem cell-derived colonoids [Figure 12C and D]. Moreover, MAPK inhibitors U0126 or PD98059 inhibited rapamycin and starvation-induced increase in occludin levels in normal human colon explants [Figure 12E and F] and occludin immunofluorescence in the colonoids [Figure 12C and D], respectively. Finally, in functional studies on Ussing chambers, rapamycin reduced paracellular inulin flux in the normal human colonic mucosa, which was prevented by both U0126 and PD98059 treatment [Figure 12G]. Together, these data show that autophagy induces upregulation of occludin in human colonic tissues and enhances the paracellular TJ barrier, in an MAPK-dependent manner.

4. Discussion

We have previously reported that nutrient starvation-induced autophagy reduces intestinal epithelial TJ permeability and enhances TJ barrier function via degradation of the cation-selective, pore-forming TJ protein claudin-2.[8,9] Here we show a novel role of the autophagy pathway, which is traditionally thought to be degradative, in selective preservation of

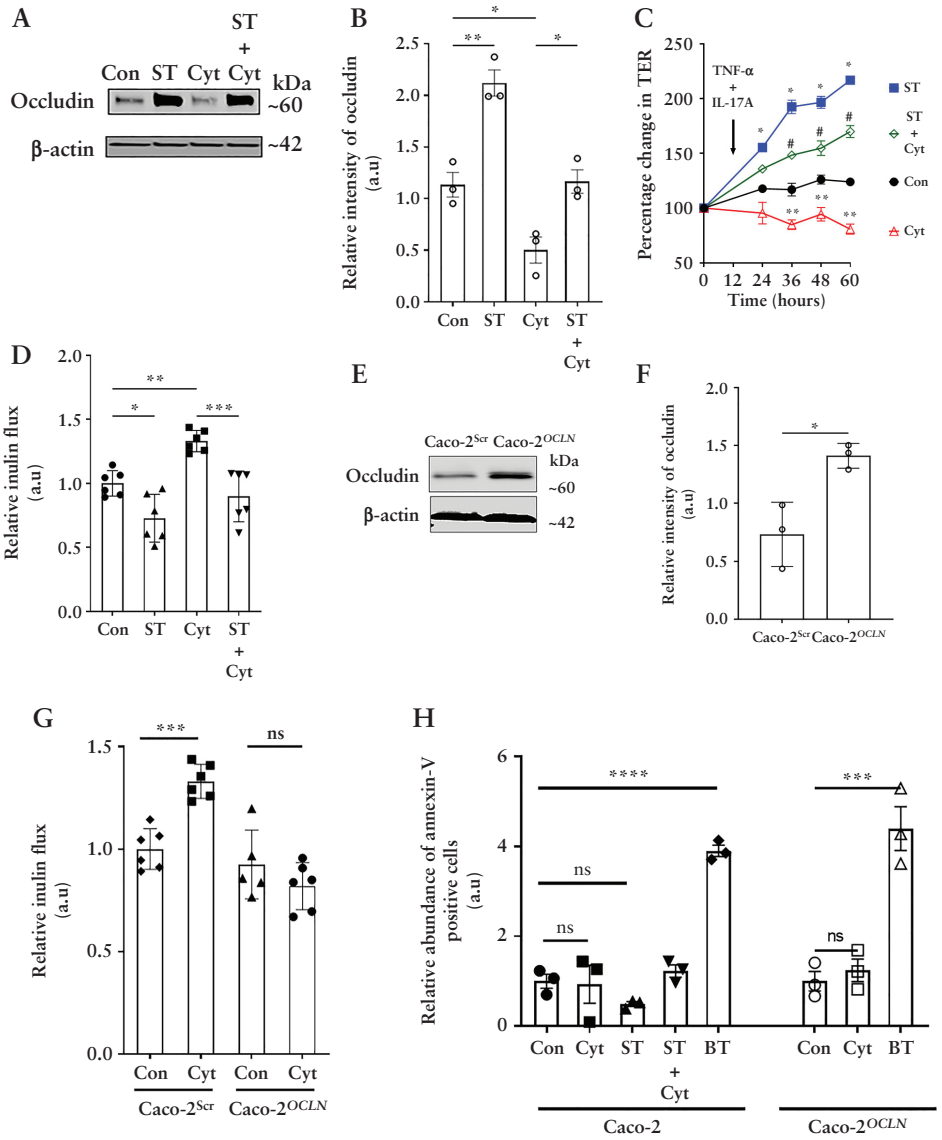

Figure 9. Autophagy-mediated and exogenous occludin overexpression protects against inflammation-induced barrier loss. [A] Basolateral treatment of Caco-2 cell monolayers with a cocktail of inflammatory cytokines [Cyt] mimicking the inflammatory state (IFN-γ [20 ng/mL], TNF-α [10 ng/mL] and IL-17A [50 ng/mL]) induced reduction in occludin levels which was inhibited by starvation. [B] Densitometric quantification of occludin from panel A. Blot and graph representative of three independent experiments. [C] Starvation protected Caco-2 cell monolayers from Cyt treatment-induced drop in TER. Student's *t*-test. *, $p < 0.05$ Con vs ST; **, $p < 0.05$ Con vs Cyt; #, $p < 0.05$ Cyt vs ST + Cyt. Representative of three independent experiments. [D] Starvation protected Caco-2 cell monolayers from IFN-γ, TNF-α and IL-17A [Cyt] treatment-induced increase in paracellular inulin flux. $n = 4$. [E] Baseline occludin levels in empty vector [Caco-2^{Scr}] and occluding-overexpressing [Caco-2^{OCLN}] vector-transfected Caco-2 cells. [F] Quantification of occludin in panel C. Blot and densitometric quantification from three independent experiments. [G] Occludin overexpression protected against the cytokine-induced [Cyt] inulin flux. [H] Cytokine treatment did not induce apoptosis in Caco-2 or Caco-2 OCLN cells as assessed by Annexin-V staining. Butyrate [BT, 20 mM] treatment is shown as a positive control for apoptosis.[33] Student's *t*-test or one-way ANOVA with Tukey's post-hoc test. *, $p < 0.05$; **, $p < 0.01$; ***, $p < 0.001$; ****, $p < 0.0001$; ns, non-significant.

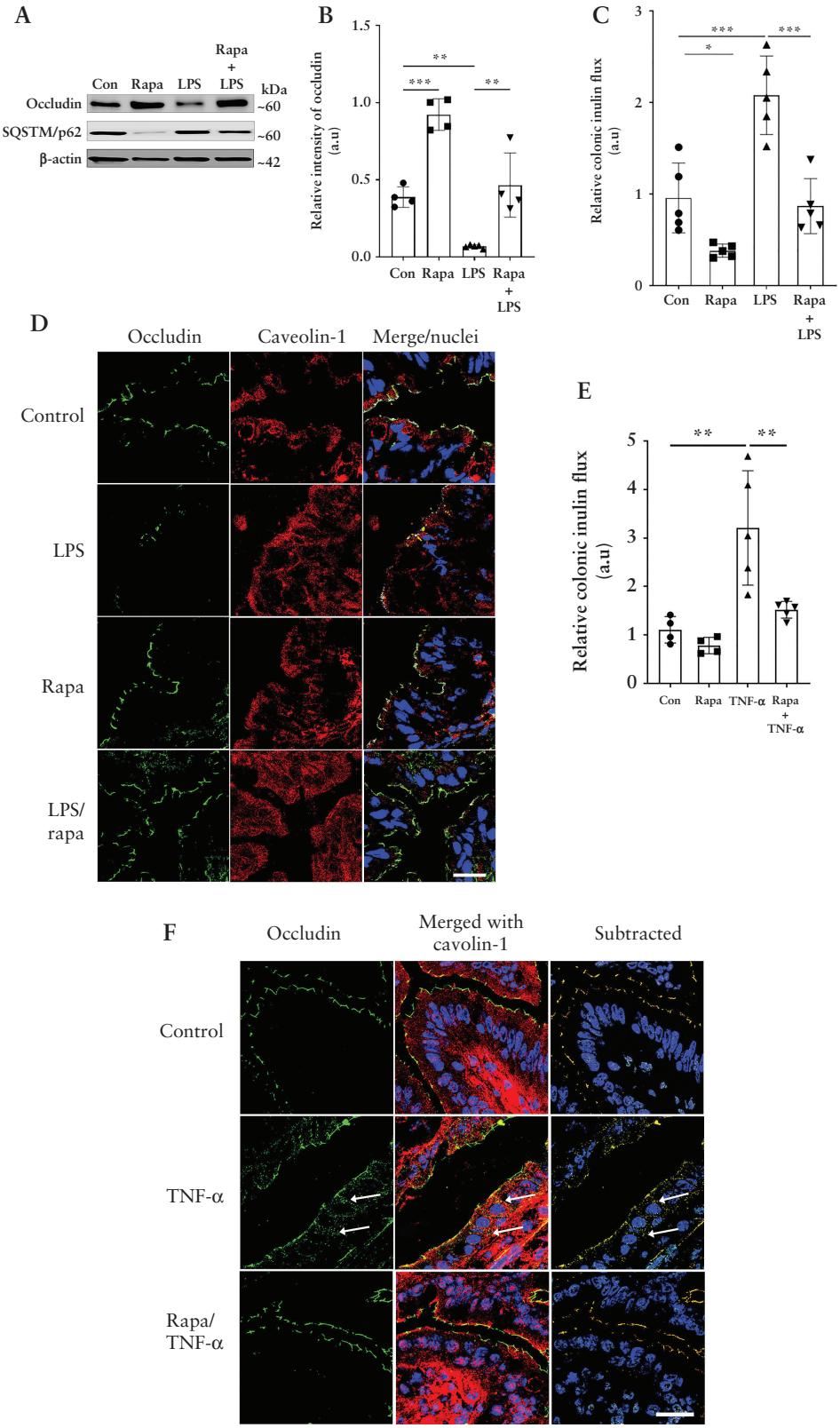

Figure 10. Autophagy protects against inflammation-induced TJ barrier loss *in vivo*. [A] Rapamycin protected against LPS [0.2 μg/kg, 16 h]-induced reduction in occludin in mouse colonocytes. Degradation of SQSTM/p62 indicates autophagy induction. [B] Quantification of occludin from panel A. $n = 6$ per group. [C] Rapamycin protected against LPS-induced increase in inulin flux. $n = 6$ per group. [D] LPS-induced loss of occludin [green] was prevented by rapamycin. Caveolin-1 [red], nuclei [blue]. White scale bar = 10 μm. [E] Rapamycin protected against TNF-α [0.2 μg/kg, 4 h]-induced loss of colonic TJ barrier. $n = 6$ per group. [F] Rapamycin prevented the TNF-α-induced increase in the association between occludin [green] and caveolin-1 [red] [white arrows, yellow colour] in WT mice. White scale bar = 10 μm. One-way ANOVA with Tukey's post-hoc test. *, $p < 0.05$; **, $p < 0.01$; ***, $p < 0.001$.

the TJ protein occludin and reduction in the paracellular permeability of macromolecules. The starvation-mediated upregulation of the barrier-forming protein occludin contrasts with its degradation-promoting effect on the pore-forming protein claudin-2 and emphasizes two distinct mechanisms through which autophagy mediates enhancement of the TJ barrier.

Our study shows that starvation-induced autophagy upregulates occludin in different epithelial cell lines, mouse and human intestinal tissue, and tissue-derived organoids, and this effect was also produced by several known pharmacological inducers of autophagy. Starvation reduced the Tyr phosphorylation and increased Thr phosphorylation of occludin, resulting in stabilization of the protein's localization to the TJs and the consequential enhancement of the paracellular barrier against macromolecular flux. On the other hand, pharmacological and genetic inhibition of the autophagy pathway prevented starvation-induced TJ barrier enhancement. We also highlight the importance of occludin in maintaining the paracellular barrier. Consistent with the previous reports,[37–39] the baseline inulin flux in the *OCLN*$^{-/-}$ cells remained unaltered, but autophagy-induced barrier enhancement was not observed in these cells. These observations agree with previous reports where mice lacking occludin had no morphological or functional differences in the TJs but showed retarded post-natal development, age-dependent barrier dysfunction and an increased propensity for gut injury, implicating that occludin is crucial for TJ barrier maintenance.[39–42] Several studies, including ours, have demonstrated that occludin is constitutively trafficked via caveolae.[11,20,43,44] Our present study demonstrates that autophagy enhances occludin levels by reducing its endocytosis from the membrane and increasing its half-life. Furthermore, we show that autophagy shunts occludin off the constitutive degradation pathway by disrupting its association with caveolin-1 and Atg-6/beclin-1. Previously, we reported that Atg-6/beclin-1 regulates constitutive degradation of occludin,[26] and our present findings suggest that engagement of beclin-1 in the autophagy pathway spares occludin from degradation.

TJ barrier composition and integrity are regulated by different kinases, and the protective role of the Ser/Thr kinases ERK-1 and ERK-2 have been established previously.[45,46] Activation of ERK-1 and 2 by the AMP-activated protein kinase [AMPK] and subsequent activation of TSC2 or their AMPK-independent activation by protein kinase C [PKC][47] is involved in promoting autophagy.[28,48] Our findings show the necessity of ERK-1 and ERK-2 activation in starvation- associated TJ barrier enhancement and occludin localization to the TJ barrier. Our data also underscore the importance of the ERK kinases in protecting occludin from degradation as, in their absence, autophagy induction failed to reduce the association of occludin with either caveolae or lysosomes, and did not protect against CSD-induced occludin endocytosis. Our study also highlights the importance of the ERK1/2 kinases in altering the phosphorylation state of occludin, which in turn determines the stability of occludin at the TJs. Based on

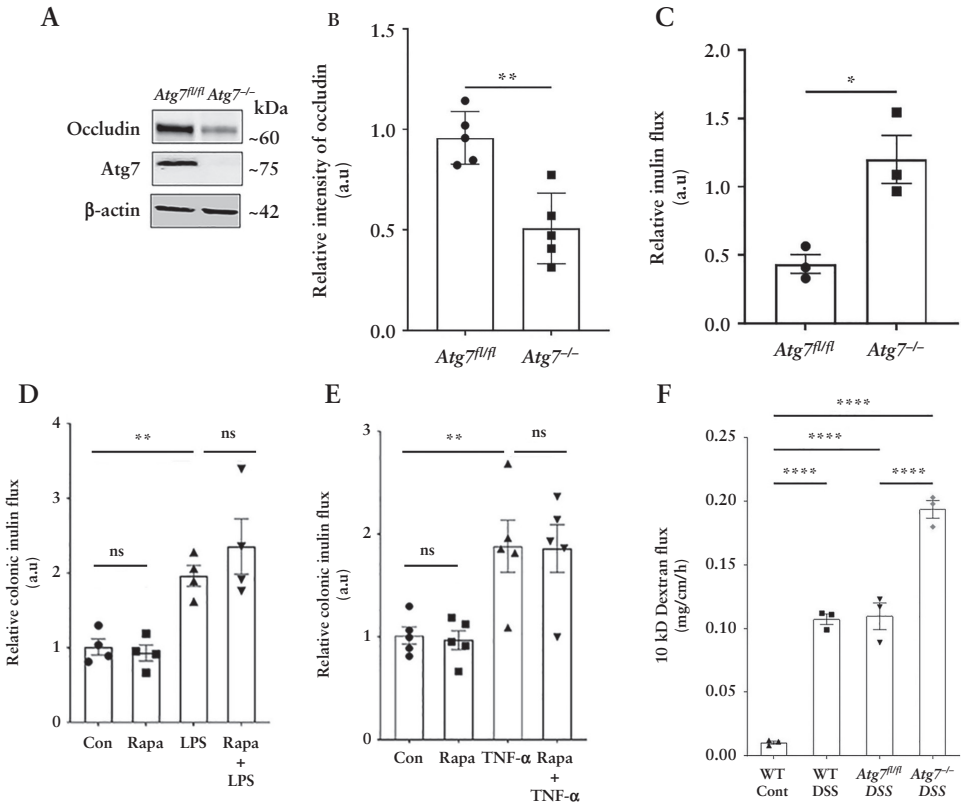

Figure 11. Rapamycin-induced protection against inflammation is autophagy-dependent. [A] Tamoxifen treatment of adult mice with Atg7 floxed and Ubc-CreERT2 alleles resulted in the loss of ATG7 protein in colonic mucosa [*Atg7*$^{-/-}$ mice] and caused a decrease in constitutive occludin levels in the colonic epithelial cells. [B] Densitometry for occludin levels in *Atg7*$^{-/-}$ mice. $n = 5$ per group. [C] Baseline colonic inulin flux in *Atg7*$^{fl/fl}$ and *Atg7*$^{-/-}$ mice. $n = 3$ per group. Rapamycin failed to prevent LPS- [D] and TNF-α [E]-induced increase in colonic inulin flux in *Atg7*$^{-/-}$ mice. $n = 4$ per group. [F] In the acute DSS colitis model, *Atg7*$^{-/-}$ mice showed markedly increased colonic inulin flux compared to *Atg7*$^{fl/fl}$ DSS and WT DSS mice. $n = 3$ per group. Student's *t*-test or one-way ANOVA with Tukey's post-hoc test. *, $p < 0.05$; **, $p < 0.01$; ***, $p < 0.001$; ****, $p < 0.0001$; ns, non-significant.

the current literature, we speculate that this altered occludin phosphorylation after autophagy induction is due to the reciprocal regulation between ERK1/2 and the c-Src kinase, which is known to facilitate the Tyr phosphorylation of occludin and compromise its TJ stability[22,49–51] and needs further investigation. In addition, though we found that ERK1/2 does not have conventional caveolin binding motifs [CBMs], non-conventional CBMs, which are also known to mediate interaction with the scaffold domain [SD] of caveolin-1, were found in both ERK1/2.[52] These observations, coupled with our data that starvation enhances the association between the ERK kinases and caveolin-1 alongside the Caco-2 protein interactome upon starvation, point to a direct role of autophagy-activated ERK1/2 kinases in preventing the association between caveolin-1 and occludin.

Occludin has been described as a critical regulator of the leak pathway, which due to its ability to allow fluid and large solute movement including luminal antigens, plays a pivotal role in the regulation of the gut mucosal immune responses and gut inflammation.[25,53,54] To understand the relevance of autophagy-mediated occludin upregulation in inflammation, we used multiple *in vitro* and *in vivo* injury models of cytokines, LPS and DSS colitis, which have previously been shown to increase gut permeability. We found that *in vitro*, autophagy induction by starvation or exogenous occludin overexpression successfully prevented the cytokine-induced increase in paracellular macromolecule permeability. This is unlike a previous report in MDCK II cells that shows depletion of the TJ barrier with overexpression of occludin during cytokine treatment,[44] possibly due to the different cell line models or the autophagy-mediated regulation of intracellular pathways including caveolin-1. Furthermore, *in vivo* observations show that autophagy induction with rapamycin in the intestine of WT, but not *Atg7*$^{-/-}$, mice protects against the disruptive effect of LPS and TNF-α on the TJ barrier. Additionally, the overall severity of DSS colitis including the

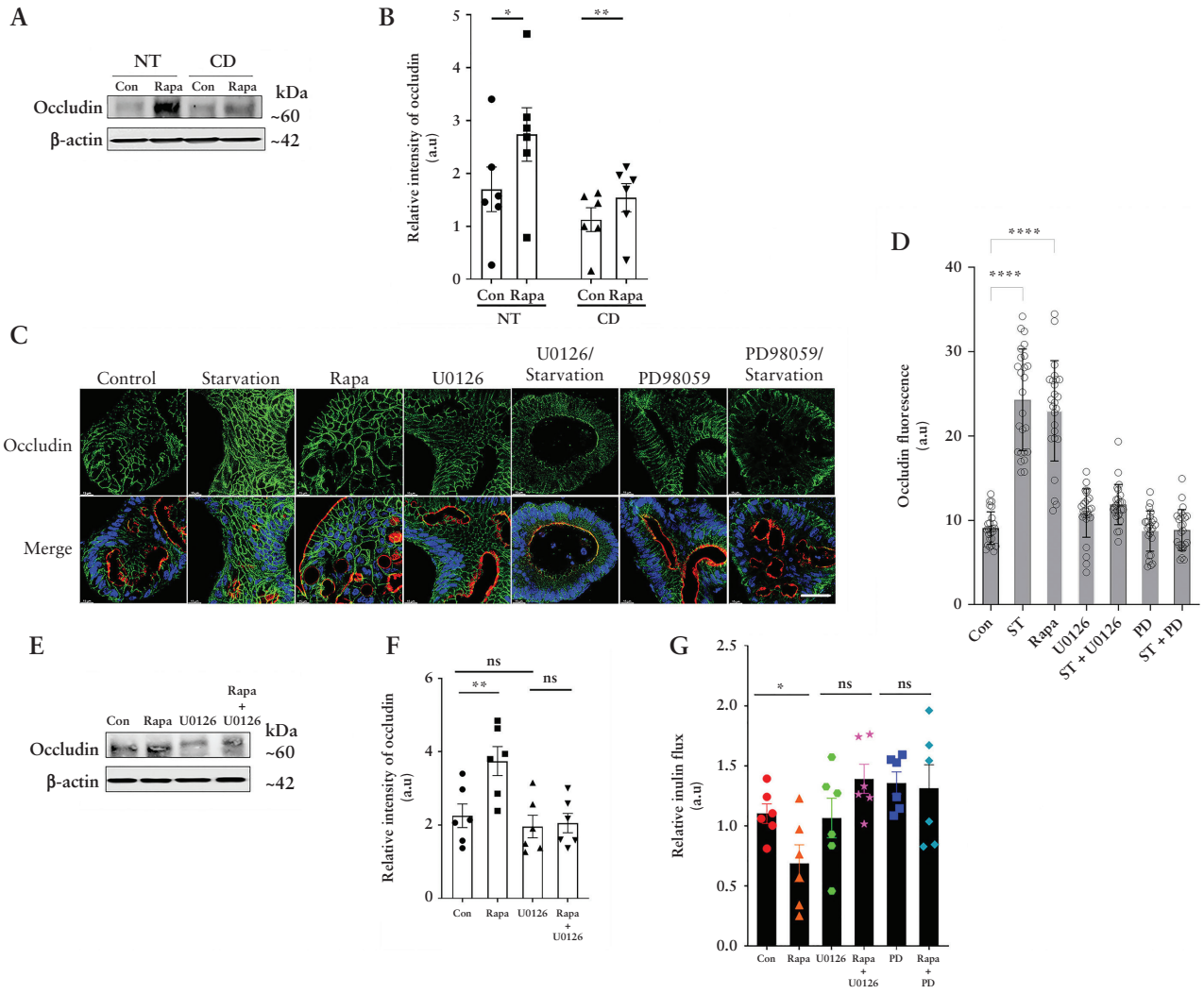

Figure 12. Autophagy enhances occludin levels in human colonic tissues in an ERK1/2-dependent mechanism. [A] Western blot for occludin from rapamycin- [300 nM] treated normal [NT] and Crohn's disease [CD] colonic mucosal tissue. [B] Quantification of occludin levels in panel A. [C] Confocal immunofluorescence for occludin [green], apical F-actin [red] and nuclei [blue] in normal human colonoids after 18 h of the indicated treatments. White scale bar = 10 μm. [D] Quantification of occludin fluorescence from panel C. Data are representative of three or more independent experiments with multiple fields captured in each. [E] Occludin levels from normal human mucosa upon rapamycin treatment with or without the ERK1/2 inhibitor U0126 [25 μM]. Inhibition of ERK1/2 prevented the rapamycin-induced upregulation of occludin levels. [F] Quantification of occludin levels in panel E. $n = 6$ per group. [G] Rapamycin-induced reduction in human colonic inulin flux was prevented upon inhibition of ERK1/2 with U0126 or PD98059. $n = 6$ per group. One-way ANOVA with Tukey's post-hoc test. *, $p < 0.05$; **, $p < 0.01$; ****, $p < 0.0001$; ns, non-significant.

colonic paracellular macromolecule flux was markedly increased in *Atg7*$^{-/-}$ mice. These observations, along with the decreased baseline occludin expression and increased colonic macromolecule flux in *Atg7*$^{-/-}$ mice, support our previous *in vitro* findings[26] that autophagy is essential for regulating constitutive occludin levels and the TJ barrier function. In addition to the *in vitro* and *in vivo* approaches using epithelial cell lines and mouse models, we show that autophagy-induction increases occludin protein levels in healthy and IBD patient-derived colonic tissues and tissue-derived organoids in an ERK1/2-dependent way.

Presently, autophagy is known to degrade several membrane proteins including amyloid precursor protein, Notch1, focal adhesions and claudin-2.[8,55–57] Thus, autophagy-mediated suppression of occludin degradation appears to be a unique function of autophagy. Occludin overexpression or promotion of occludin expression is generally known to restrict TJ barrier loss.[25,42,58,59] On the other hand, the inflamed intestinal mucosa in patients with active IBD had decreased occludin expression.[12–14] Thus, our findings of autophagy-induced upregulation of occludin are highly significant given the role of occludin in the TJ barrier, along with the defects in the TJ barrier and autophagy reported in IBD. In conclusion, our present study demonstrates a unique function of autophagy in occludin up-regulation and enhancement of the TJ barrier. Autophagy may provide a novel tool to promote epithelial integrity during intestinal inflammation.

Funding

This research work was supported in part by the National Institute of Diabetes and Digestive and Kidney Diseases grant DK100562 [P.N.], DK114024 [P.N.], DK-106072 [T.M.], National Institute of General Medical Sciences grant P20-GM-121176, and Crohn's & Colitis Foundation Award 694583 [M.N.]. The content is solely the responsibility of the authors and does not necessarily represent the official views of the funding agencies. The authors also acknowledge support from the Peter and Marshia Carlino Fund for IBD Research.

Conflict of Interest

No conflicts of interest, financial or otherwise, are declared by the author[s].

Acknowledgments

The authors thank Mr Leonard Harris and Mrs Sue Deiling of the Colorectal Diseases Biobank, Imaging cores and Animal Facility cores at the Penn State College of Medicine for their excellent technical assistance.

Author Contributions

K.S.: study design, concept, data acquisition, analysis, interpretation, manuscript writing, statistical analysis; A.S.G.: data acquisition, analysis, interpretation, technical resources; A.W.: data acquisition, manuscript writing, technical support; N.M.M.: data acquisition, technical support, ES: data acquisition, technical support, W.D.: technical resources and support; G.Y.: technical resources and interpretation; W.K.: technical and research resources, interpretation; M.N.: technical and material resources, analysis and interpretation, funding; T.M.: technical and material resources, analysis and interpretation, funding; P.N.: study conception, study design, data acquisition, analysis, interpretation, statistical analysis, manuscript writing, revision, approval, funding, study supervision, technical and material support.

Data Availability

The data underlying this article are available in the article and/or will be provided on request.

References

1 Collaborators GBDIBD. The global, regional, and national burden of inflammatory bowel disease in 195 countries and territories, 1990–2017: a systematic analysis for the Global Burden of Disease Study 2017. *Lancet Gastroenterol Hepatol* 2020;**5**:17–30.
2 Pastorelli L, De Salvo C, Mercado J, Vecchi M, Pizarro T. Central role of the gut epithelial barrier in the pathogenesis of chronic intestinal inflammation: lessons learned from animal models and human genetics. *Front Immunol* 2013;**4**:280.
3 Turner JR. Intestinal mucosal barrier function in health and disease. *Nat Rev Immunol* 2009;**9**:799–809.
4 Levine B, Kroemer G. Autophagy in the pathogenesis of disease. *Cell* 2008;**132**:27–42.
5 Deretic V, Saitoh T, Akira S. Autophagy in infection, inflammation and immunity. *Nat Rev Immunol* 2013;**13**:722–37.
6 Birgisdottir AB, Johansen T. Autophagy and endocytosis – interconnections and interdependencies. *J Cell Sci* 2020;**133**: jcs228114.
7 Nighot P, Ma T. Endocytosis of intestinal tight junction proteins: in time and space. *Inflamm Bowel Dis* 2021;**27**:283–90.
8 Ganapathy AS, Saha K, Suchanec E, *et al*. AP2M1 mediates autophagy-induced CLDN2 (claudin 2) degradation through endocytosis and interaction with LC3 and reduces intestinal epithelial tight junction permeability. *Autophagy* 2022;**18**:2086–103.
9 Nighot PK, Hu CA, Ma TY. Autophagy enhances intestinal epithelial tight junction barrier function by targeting claudin-2 protein degradation. *J Biol Chem* 2015;**290**:7234–46.
10 Nighot P, Ma T. Role of autophagy in the regulation of epithelial cell junctions. *Tissue Barriers* 2016;**4**:e1171284.
11 Cummins PM. Occludin: one protein, many forms. *Mol Cell Biol* 2012;**32**:242–50.
12 Zeissig S, Burgel N, Gunzel D, *et al*. Changes in expression and distribution of claudin 2, 5 and 8 lead to discontinuous tight junctions and barrier dysfunction in active Crohn's disease. *Gut* 2007;**56**:61–72.
13 Heller F, Florian P, Bojarski C, *et al*. Interleukin-13 is the key effector Th2 cytokine in ulcerative colitis that affects epithelial tight junctions, apoptosis, and cell restitution. *Gastroenterology* 2005;**129**:550–64.
14 Schmitz H, Barmeyer C, Fromm M, *et al*. Altered tight junction structure contributes to the impaired epithelial barrier function in ulcerative colitis. *Gastroenterology* 1999;**116**:301–9.
15 Nighot PK, Blikslager AT. Chloride channel ClC-2 modulates tight junction barrier function via intracellular trafficking of occludin. *Am J Physiol Cell Physiol* 2012;**302**:C178–87.
16 Nighot M, Ganapathy AS, Saha K, *et al*. Matrix metalloproteinase MMP-12 promotes macrophage transmigration across intestinal epithelial tight junctions and increases severity of experimental colitis. *J Crohns Colitis* 2021;**15**:1751–65.
17 Karsli-Uzunbas G, Guo JY, Price S, *et al*. Autophagy is required for glucose homeostasis and lung tumor maintenance. *Cancer Discov* 2014;**4**:914–27.
18 Nighot P, Al-Sadi R, Rawat M, Guo S, Watterson DM, Ma T. Matrix metalloproteinase 9-induced increase in intestinal epithelial tight junction permeability contributes to the severity of experimental DSS colitis. *Am J Physiol Gastrointest Liver Physiol* 2015;**309**:G988–97.

19 Park D, Jeong H, Lee MN, *et al*. Resveratrol induces autophagy by directly inhibiting mTOR through ATP competition. *Sci Rep* 2016;**6**:21772.
20 Renna M, Jimenez-Sanchez M, Sarkar S, Rubinsztein DC. Chemical inducers of autophagy that enhance the clearance of mutant proteins in neurodegenerative diseases. *J Biol Chem* 2010;**285**:11061–7.
21 Shaw RJ, Lamia KA, Vasquez D, *et al*. The kinase LKB1 mediates glucose homeostasis in liver and therapeutic effects of metformin. *Science* 2005;**310**:1642–6.
22 Rao R. Occludin phosphorylation in regulation of epithelial tight junctions. *Ann N Y Acad Sci* 2009;**1165**:62–8.
23 Shen L, Weber CR, Raleigh DR, Yu D, Turner JR. Tight junction pore and leak pathways: a dynamic duo. *Annu Rev Physiol* 2010;**73**:283–309.
24 Buschmann MM, Shen L, Rajapakse H, *et al*. Occludin OCEL-domain interactions are required for maintenance and regulation of the tight junction barrier to macromolecular flux. *Mol Biol Cell* 2013;**24**:3056–68.
25 Marchiando AM, Shen L, Graham WV, *et al*. Caveolin-1-dependent occludin endocytosis is required for TNF-induced tight junction regulation in vivo. *J Cell Biol* 2010;**189**:111–26.
26 Wong M, Ganapathy AS, Suchanec E, Laidler L, Ma T, Nighot P. Intestinal epithelial tight junction barrier regulation by autophagy-related protein ATG6/beclin 1. *Am J Physiol Cell Physiol* 2019;**316**:C753–65.
27 Morimoto S, Nishimura N, Terai T, *et al*. Rab13 mediates the continuous endocytic recycling of occludin to the cell surface. *J Biol Chem* 2005;**280**:2220–8.
28 Wang J, Whiteman MW, Lian H, *et al*. A non-canonical MEK/ERK signaling pathway regulates autophagy via regulating Beclin 1. *J Biol Chem* 2009;**284**:21412–24.
29 Basuroy S, Seth A, Elias B, Naren AP, Rao R. MAPK interacts with occludin and mediates EGF-induced prevention of tight junction disruption by hydrogen peroxide. *Biochem J* 2006;**393**:69–77.
30 Strober W, Fuss IJ. Proinflammatory cytokines in the pathogenesis of inflammatory bowel diseases. *Gastroenterology* 2011;**140**:1756–67.
31 Monteleone I, Pallone F, Monteleone G. Interleukin-23 and Th17 cells in the control of gut inflammation. *Mediators Inflamm* 2009;297645.
32 Kuo WT, Shen L, Zuo L, *et al*. Inflammation-induced occludin downregulation limits epithelial apoptosis by suppressing caspase-3 expression. *Gastroenterology* 2019;**157**:1323–37.
33 Ruemmele FM, Schwartz S, Seidman EG, Dionne S, Levy E, Lentze MJ. Butyrate induced Caco-2 cell apoptosis is mediated via the mitochondrial pathway. *Gut* 2003;**52**:94–100.
34 Feng Y, Teitelbaum DH. Tumour necrosis factor-induced loss of intestinal barrier function requires TNFR1 and TNFR2 signalling in a mouse model of total parenteral nutrition. *J Physiol* 2013;**591**:3709–23.
35 Watari A, Sakamoto Y, Hisaie K, *et al*. Rebeccamycin attenuates TNF-α-induced intestinal epithelial barrier dysfunction by inhibiting myosin light chain kinase production. *Cell Physiol Biochem* 2017;**41**:1924–34.
36 Tsuboi K, Nishitani M, Takakura A, Imai Y, Komatsu M, Kawashima H. Autophagy protects against colitis by the maintenance of normal gut microflora and secretion of mucus. *J Biol Chem* 2015;**290**:20511–26.
37 Balda MS, Whitney JA, Flores C, Gonzalez S, Cereijido M, Matter K. Functional dissociation of paracellular permeability and transepithelial electrical resistance and disruption of the apical–basolateral intramembrane diffusion barrier by expression of a mutant tight junction membrane protein. *J Cell Biol* 1996;**134**:1031–49.
38 McCarthy KM, Skare IB, Stankewich MC, *et al*. Occludin is a functional component of the tight junction. *J Cell Sci* 1996;**109**:2287–98.
39 Mir H, Meena AS, Chaudhry KK, *et al*. Occludin deficiency promotes ethanol-induced disruption of colonic epithelial junctions, gut barrier dysfunction and liver damage in mice. *Biochim Biophys Acta* 2016;**1860**:765–74.
40 Ronaghan NJ, Shang J, Iablokov V, *et al*. The serine protease-mediated increase in intestinal epithelial barrier function is dependent on occludin and requires an intact tight junction. *Am J Physiol Gastrointest Liver Physiol* 2016;**311**:G466–79.
41 Singh V, Gowda CP, Singh V, *et al*. The mRNA-binding protein IGF2BP1 maintains intestinal barrier function by up-regulating occludin expression. *J Biol Chem* 2020;**295**:8602–12.
42 Chu Y, Zhu Y, Zhang Y, *et al*. Tetrandrine attenuates intestinal epithelial barrier defects caused by colitis through promoting the expression of occludin via the AhR-miR-429 pathway. *FASEB J* 2021;**35**:e21502.
43 Fletcher SJ, Iqbal M, Jabbari S, Stekel D, Rappoport JZ. Analysis of occludin trafficking, demonstrating continuous endocytosis, degradation, recycling and biosynthetic secretory trafficking. *PLoS One* 2014;**9**:e111176.
44 Van Itallie CM, Fanning AS, Holmes J, Anderson JM. Occludin is required for cytokine-induced regulation of tight junction barriers. *J Cell Sci* 2010;**123**:2844–52.
45 Kim B, Breton S. The MAPK/ERK-signaling pathway regulates the expression and distribution of tight junction proteins in the mouse proximal epididymis. *Biol Reprod* 2016;**94**:22.
46 Samak G, Aggarwal S, Rao RK. ERK is involved in EGF-mediated protection of tight junctions, but not adherens junctions, in acetaldehyde-treated Caco-2 cell monolayers. *Am J Physiol Gastrointest Liver Physiol* 2011;**301**:G50–9.
47 Mandic M, Misirkic Marjanovic M, Vucicevic L, *et al.* MAP kinase-dependent autophagy controls phorbol myristate acetate-induced macrophage differentiation of HL-60 leukemia cells. *Life Sci* 2022;**297**:120481.
48 Ugland H, Naderi S, Brech A, Collas P, Blomhoff HK. cAMP induces autophagy via a novel pathway involving ERK, cyclin E and Beclin 1. *Autophagy* 2011;**7**:1199–211.
49 Basuroy S, Sheth P, Kuppuswamy D, Balasubramanian S, Ray RM, Rao RK. Expression of kinase-inactive c-Src delays oxidative stress-induced disassembly and accelerates calcium-mediated reassembly of tight junctions in the Caco-2 cell monolayer. *J Biol Chem* 2003;**278**:11916–24.
50 Chelakkot C, Ghim J, Rajasekaran N, *et al*. Intestinal epithelial cell-specific deletion of PLD2 alleviates DSS-induced colitis by regulating occludin. *Sci Rep* 2017;**7**:1573.
51 Tsukita S, Oishi K, Akiyama T, Yamanashi Y, Yamamoto T, Tsukita S. Specific proto-oncogenic tyrosine kinases of src family are enriched in cell-to-cell adherens junctions where the level of tyrosine phosphorylation is elevated. *J Cell Biol* 1991;**113**:867–79.
52 Byrne DP, Dart C, Rigden DJ. Evaluating caveolin interactions: do proteins interact with the caveolin scaffolding domain through a widespread aromatic residue-rich motif? *PLoS One* 2012;**7**:e44879.
53 Su L, Shen L, Clayburgh DR, *et al*. Targeted epithelial tight junction dysfunction causes immune activation and contributes to development of experimental colitis. *Gastroenterology* 2009;**136**:551–63.
54 Zuo L, Kuo W-T, Turner JR. Tight junctions as targets and effectors of mucosal immune homeostasis. *Cell Mol Gastroenterol Hepatol* 2020;**10**:327–40.
55 Tian Y, Chang JC, Fan EY, Flajolet M, Greengard P. Adaptor complex AP2/PICALM, through interaction with LC3, targets Alzheimer's APP-CTF for terminal degradation via autophagy. *Proc Natl Acad Sci U S A* 2013;**110**:17071–6.
56 Wu X, Fleming A, Ricketts T, *et al*. Autophagy regulates Notch degradation and modulates stem cell development and neurogenesis. *Nat Commun* 2016;**7**:10533.
57 Kenific CM, Stehbens SJ, Goldsmith J, *et al*. NBR1 enables autophagy-dependent focal adhesion turnover. *J Cell Biol* 2016;**212**:577–90.
58 Nighot PK, Leung L, Ma TY. Chloride channel ClC-2 enhances intestinal epithelial tight junction barrier function via regulation of caveolin-1 and caveolar trafficking of occludin. *Exp Cell Res* 2017;**352**:113–22.
59 Chen Y, Zhang HS, Fong GH, *et al*. PHD3 stabilizes the tight junction protein occludin and protects intestinal epithelial barrier function. *J Biol Chem* 2015;**290**:20580–9.